Protein crystals make it big at electrode surfaces

Barry R. Silver*[a] and Patrick R. Unwin*[b]

Received (in Cambridge, UK) 17th June 2008, Accepted 7th August 2008
First published as an Advance Article on the web 10th September 2008
DOI: 10.1039/b810226k

Enhanced and rapid growth of lysozyme crystals at the surface of a platinum electrode, using an applied current and a simplified crystallizing solution, is demonstrated.

The formation of protein crystals with good X-ray diffraction quality is a fundamental step in the elucidation of protein structure *via* X-ray crystallography.[1] Methods used to obtain protein crystals are largely trial and error; indeed the precise mechanisms by which many protein crystals nucleate and grow is not completely understood.[2] The nucleation and growth of lysozyme crystals from homogeneous solution has been studied over a wide range of pH and solution conditions.[3–5] It has been shown previously that low pH promotes the nucleation process, but leads to the formation of a large number of relatively small crystals.[3,6] Here, we show how electrochemistry can be used to control and enhance the growth of protein crystals, exemplified through studies of the protein lysozyme. The time to achieve significant growth was much reduced compared to conventional crystal growth methods. In addition, the composition of the crystallizing solution used was much simplified, compared to commonly used buffer, protein and precipitant mixes. The approach herein may be generic for producing high quality protein crystals for X-ray diffraction studies. Furthermore, the approach described provides a platform for fundamental studies of the nucleation, growth and dissolution of protein crystals on substrates.

The application of both internal and external electrical fields is a relatively new concept which has been used to influence the behaviour of protein crystallizing solutions.[4] Our particular experimental set-up involves a simple two-electrode galvanostatic system which enables an electrical current to be passed through a lysozyme crystallizing solution. In contrast to conventional lysozyme crystallization approaches, the solution used herein was not buffered. The omission, of what is conventionally an acetate buffer,[3–11] was to allow the creation a zone of relatively low pH in the vicinity of one electrode within our electrochemical cell. This contrasts with other work using electrical currents for protein crystallization, where pH changes are rendered negligible *via* the addition of buffer.[4,8,12]

The crystallizing solution was made from equal aliquots of 75 mg ml^{-1} lysozyme (Sigma-Aldrich, UK) and 8.73 (w/v)% NaCl. Both constituents were dissolved in Milli-Q water and the solution was centrifuged for 30 min. Typically, an anodic current of 5 μA was applied to a 2 mm diameter platinum disc electrode using a galvanostat with a platinum wire serving as a counter electrode (potential in the range 1.5 to 1.8 V). For comparison with the electrochemical method, two types of control experiment were carried out. The first consisted of crystallizing solution without applied current (control A) and a second consisted of crystallizing solution with a pH of 3.5 (control B). This second control was important and necessary, as it allowed us to approximate conditions generated electrochemically at the anode surface, but the low pH was uniform throughout the solution. In all cases, the solutions were left for a period of up to 2 h.

The significant effect of the applied anodic current is illustrated in Fig. 1. Large crystals were obtained, with sizes in excess of 180 μm commonly seen after 2 h. The experiment with no applied current (control A) exhibits a higher number of crystals, but with sizes of approximately 80 μm common. The second control (control B) shows even more nucleation, with crystal sizes of approximately 20–30 μm obtained after 2 h.

Further experiments were conducted in which lysozyme was conjugated to the fluorescent succinimidyl ester, Alexa Flour 488 (Invitrogen). The solution contained 0.5% by volume of the labelled protein. The crystals obtained during the electrochemical crystallization process were visualised *in situ* using a confocal laser scanning microscope (CLSM, model Zeiss LM 510) at various time periods using an excitation wavelength of 488 nm, with detection of emission above 505 nm.

Crystal sizes obtained using the part-fluorescently labelled crystallizing solution were similar both in magnitude and habit to those obtained using the unlabelled solution. The fluorescently labelled lysozyme allowed ready visualization of the crystals which had nucleated on the electrode surface, as well as those which had nucleated and grown on the surrounding insulating Bakelite material. Fig. 2 clearly shows that much larger crystals are formed on the electrode surface compared to the insulating material after 45 min of applied current.

Since an anodic current was applied to the electrode, we expected the pH to change in the solution immediately above the electrode surface[13] due to the oxidation of water.

Fig. 1 Lysozyme crystals formed at an electrode surface after 2 h. From left to right: 5 μA applied current; no current; and no current with solution pH of 3.5. Scale bar shown is 350 μm.

[a] *Molecular Organisation and Assembly in Cells Doctoral Training Centre (MOAC DTC), Coventry House, University of Warwick, Coventry, UK CV4 7AL. E-mail: b.r.silver@warwick.ac.uk*
[b] *Department of Chemistry, University of Warwick, Coventry, UK CV4 7AL. E-mail: p.r.unwin@warwick.ac.uk; Fax: +44 (0) 2476 524112; Tel: +44 (0) 2476 523264*

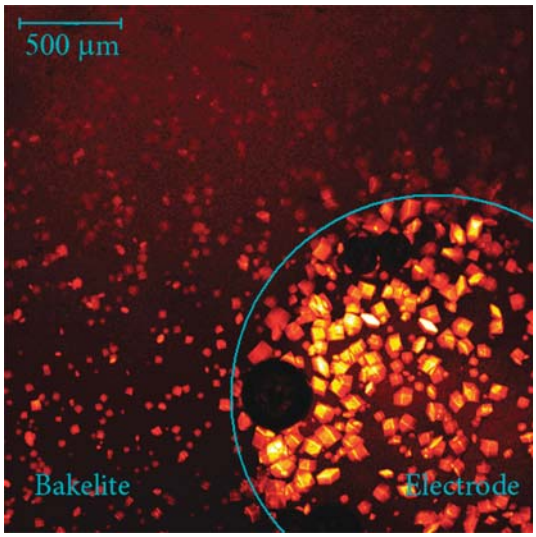

Fig. 2 *In situ* laser scanning confocal micrograph of the electrode interface and the surrounding layer of insulating Bakelite after 45 min of applied current. The blue line indicates the interface between the electrode and the surrounding insulating material. Dark circles within the blue line are oxygen bubbles formed *via* electrolysis.

$$2H_2O(l) \rightarrow O_2(g) + 4H^+ + 4e^- \qquad (1)$$

The evolution of oxygen is evident in Fig. 2, while the extent of the pH gradient in the vicinity of the active surface of the electrode was visualised using the unlabelled crystallizing solution, described herein, but with the addition of 10 μM fluorescein. Fluorescein is a commonly used fluorophore in CLSM studies which exhibits a pH-sensitive fluorescence signal.[13,14] The fluorescence signal increases in aqueous solution from pH ~ 5 to a maximum as the pH rises above pH ~ 7.[13] With the same anodic electrochemical conditions, the solution above the electrode surface was monitored *via* z-stack imaging with CLSM. Fig. 3 demonstrates the extent of the pH gradient above the electrode surface, as reflected in the fluorescence signal. The white area in Fig. 3 was indicative of the fluorescent intensity of the bulk solution (pH = 6.5) and was colour saturated, *via* imaging software, in order to highlight the pH gradient that had developed below it. An approximate value for the pH at the electrode surface may be deduced by assuming a linear proton concentration gradient and noting that bulk solution is recovered at a distance, $\delta \sim 300$ μm, as seen in Fig. 3. This distance is of the order of the Nernst diffusion layer as measured at macroscopic electrodes.[15] The approximate pH at the electrode surface may be deduced from:

$$i = \frac{nFAD(C^* - C^\delta)}{\delta} \qquad (2)$$

where $n = 1$ is the number of electrons passed per proton generated (eqn (1)), F is the Faraday constant (96 500 C mol^{-1}), A is the electrode area (0.0314 cm^2), D is the proton diffusion coefficient (7.5×10^{-5} cm^2 s^{-1}), C^* is the concentration of protons at the electrode surface, C^δ is the proton concentration at boundary layer (pH ~ 6.5), δ is the boundary layer thickness and i is the applied current. We have assumed the dominant electrochemical process to be as defined in eqn (1). Previous studies at similar current densities have shown this to be valid[13] and hence an approximate pH for the electrode surface is 3.2.

By tuning the magnitude of the applied current we found that both lysozyme crystal 'growth' and 'dissolution' could be promoted. The 'dissolution' regime was established when an anodic current of 12 μA (or greater) was applied. Growth and subsequent dissolution of lysozyme crystals is illustrated in Fig. 4, which shows changes in the fluorescent intensity at the electrode surface for a fluorescently-labelled lysozyme crystallizing solution as the applied current was varied. The fluorescence intensity was monitored for 30 min of 'normal' growth with a 5 μA current. The resulting fluorescence intensity at this time was used for background subtraction. The fluorescence intensity for subsequent images was taken over the entire image area. The 5 μA current was applied for a further 1777 s and the fluorescence intensity increased approximately linearly with time, indicative of crystal growth. From 1777 s to 1924 s, 12 μA was applied and the intensity decreased slightly, indicating loss of material from the electrode due to dissolution. The application of 5 μA current between 1924 s and 2649 s caused growth to resume, but at 2649 s, a current of 20 μA caused rapid dissolution and some physical

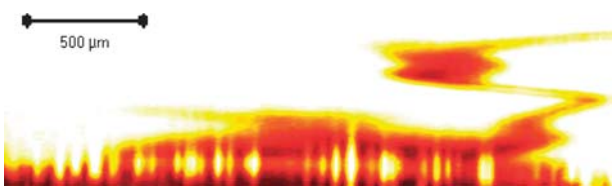

Fig. 3 Fluorescence intensity map perpendicular to the 2 mm diameter platinum disc electrode (5 μA applied). White areas indicate a pH ≥ 6.5 whilst darker areas are pH < 5. Elongated white areas on the electrode surface are lysozyme crystals which have incorporated fluorophore during growth.

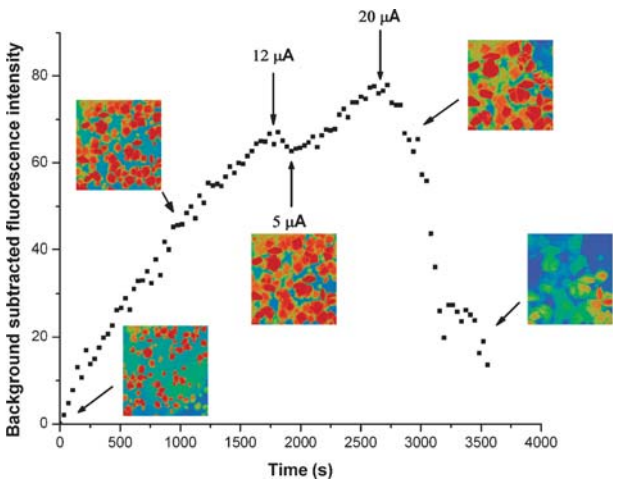

Fig. 4 Time dependence of fluorescence intensity at the electrode surface as a result of growth and dissolution of fluorescently labelled lysozyme crystals. From 0–1777 s, 5 μA current was applied. The current was then switched to 12 μA from 1777–1924 s and dissolution was seen. From 1924–2649 s 5 μA was again applied and growth resumed. For 2649 s onwards a current of 20 μA was applied and rapid dissolution resulted. *In situ* CLSM images at several times are shown (not background subtracted, area shown 550 μm × 550 μm).

removal of crystals from the surface due to oxygen bubble formation. This resulted in a sharp decrease in fluorescence intensity.

Crystal growth rates are a function of supersaturation.[5] The lower pH in the vicinity of the electrode, when 5 μA current was applied, decreases the protein solubility, leading to a higher degree of supersaturation. This increases the driving force for crystal growth, but this is restricted to a thin zone close to the electrode. This limits the number of nuclei that form, resulting in the rapid growth of large crystals. Nucleation and growth in bulk solution occurs more slowly. Thus, as protein is depleted at the electrode by crystal growth, a concentration gradient is established which supplies the electrode surface region with a high flux of soluble protein, ensuring the growth of large crystals. This effect, which is not seen in conventional bulk solution systems, is a consequence of the pH gradient effectively imposing a gradient of protein concentration at the electrode/solution interface. The interpretation of the results is further supported by previous work[7] which noted that large single crystals grew in a narrow range of 2.5–3 times the protein solubility. pH-solubility data[16] suggest the electrode surface is within this narrow supersaturation range. Note that the increase in supersaturation at the electrode does not lead to a large crystal number observed in conventional studies[3,17,18] and seen in the control B experiment (Fig. 1).

As reported, rapid growth of crystals was observed using anodic currents ranging from $\approx$4 μA to $\approx$10 μA in our apparatus which correspond to current densities of approximately 1.3–3.1 A m^{-2}. At higher applied current, a dissolution process was observed. This may indicate higher solubility of the protein crystals, direct attack by protons or minor side products of electrolysis (*e.g.* Cl_2). Application of cathodic currents to the disc electrode of the same magnitude (4–10 μA) resulted in mass 'precipitation' of protein after a few minutes with no crystals observed.

Whilst the results herein are immediately applicable to the control of lysozyme crystallization, it may be possible to use this technique to crystallize other proteins. Lysozyme has a basic isoelectric point of $\approx$10.5,[11] while many other proteins possess a mid-range isoelectric point and could show an ability to grow under both cathodic and anodic current regimes.

In summary, we have demonstrated that electrolysis is a powerful new approach for promoting the enhanced growth of lysozyme crystals on the surface of a platinum electrode. Furthermore, by tuning the magnitude of the applied current, it is possible to promote either the growth or dissolution of lysozyme crystals dynamically. This simple system provides a platform for fundamental studies of crystal growth/dissolution using other techniques (*e.g.* high resolution *in situ* microscopies). Further work is underway to apply this technique to other globular proteins.

We are grateful to Mr L. Butcher for manufacturing some of the apparatus. Funding *via* an EPSRC studentship through the MOAC Doctoral Training Centre is gratefully acknowledged by BS. We also acknowledge the assistance of Ms A. Hewison who conducted preliminary crystallization studies with this apparatus. Some of the microscopy equipment was kindly provided by the Advantage West Midlands Hydrogen-Energy initiative and we gratefully acknowledge access.

Notes and references

1 E. Nieto-Mendoza, B. A. Frontana-Uribe, G. Sazaki and A. Moreno, *J. Cryst. Growth*, 2005, **275**, 1437–1446.
2 N. E. Chayen and E. Saridakis, *Nat. Methods*, 2008, **5**, 147–153.
3 R. A. Judge, R. S. Jacobs, T. Frazier, E. H. Snell and M. L. Pusey, *Biophys. J.*, 1999, **77**, 1585–1593.
4 M. I. Al-Haq, E. Lebrasseur, H. Tsuchiya and T. Torii, *Crystallogr. Rev.*, 2007, **13**, 29–64.
5 I. Yoshizaki, T. Sato, N. Igarashi, M. Natsuisaka, N. Tanaka, H. Komatsu and S. Yoda, *Acta Crystallogr., Sect. D: Biol. Crystallogr.*, 2001, **57**, 1621–1629.
6 G. Alderton and H. L. Fevold, *J. Biol. Chem.*, 1946, **164**, 1–5.
7 M. Ataka and S. Tanaka, *Biopolymers*, 1986, **25**, 337–350.
8 A. Moreno and G. Sazaki, *J. Cryst. Growth*, 2004, **264**, 438–444.
9 M. Taleb, C. Didierjean, C. Jelsch, J. P. Mangeot and A. Aubry, *J. Cryst. Growth*, 2001, **232**, 250–255.
10 M. Taleb, C. Didierjean, C. Jelsch, J. P. Mangeot, B. Capelle and A. Aubry, *J. Cryst. Growth*, 1999, **200**, 575–582.
11 J. M. P. H. W. B. Ying-Chou Shih, *Biotechnol. Bioeng.*, 1992, **40**, 1155–1164.
12 G. Sazaki, A. Moreno and K. Nakajima, *J. Cryst. Growth*, 2004, **262**, 499–502.
13 N. C. Rudd, S. Cannan, E. Bitziou, I. Ciani, A. L. Whitworth and P. R. Unwin, *Anal. Chem.*, 2005, **77**, 6205–6217.
14 E. Bitziou, N. C. Rudd, M. A. Edwards and P. R. Unwin, *Anal. Chem.*, 2006, **78**, 1435–1443.
15 C. Amatore, S. Szunerits, L. Thouin and J.-S. Warkocz, *J. Electroanal. Chem.*, 2001, **500**, 62–70.
16 E. L. Forsythe, A. Nadarajah and M. L. Pusey, *Acta Crystallogr., Sect. D: Biol. Crystallogr.*, 1999, **55**, 1005–1011.
17 J. W. Mullin, *Crystallization*, Butterworth/Heineman, Oxford, England, 3rd edn, 1993.
18 R. Boistelle and J. P. Astier, *J. Cryst. Growth*, 1988, **90**, 14–30.